

## Analysis of nonlinear ship-induced 3d wave fields using nonlinear fourier transforms

Zhang, H.; Wahls, S.; Brühl, M.

**Publication date**

2021

**Document Version**

Final published version

**Citation (APA)**

Zhang, H., Wahls, S., & Brühl, M. (2021). *Analysis of nonlinear ship-induced 3d wave fields using nonlinear fourier transforms*. Paper presented at Coastal Dynamics Conference 2021, Delft, Netherlands.

**Important note**

To cite this publication, please use the final published version (if applicable).  
Please check the document version above.

**Copyright**

Other than for strictly personal use, it is not permitted to download, forward or distribute the text or part of it, without the consent of the author(s) and/or copyright holder(s), unless the work is under an open content license such as Creative Commons.

**Takedown policy**

Please contact us and provide details if you believe this document breaches copyrights.  
We will remove access to the work immediately and investigate your claim.

## ANALYSIS OF NONLINEAR SHIP-INDUCED 3D WAVE FIELDS USING NONLINEAR FOURIER TRANSFORMS

H. Zhang, S. Wahls and M. Brühl

Delft Center for Systems and Control (DCSC), Faculty of Mechanical, Maritime and Materials Engineering (3mE), Delft University of Technology, Mekelweg 2, 2628 CD Delft, The Netherlands. [H.Zhang-16@tudelft.nl](mailto:H.Zhang-16@tudelft.nl); [s.wahls@tudelft.nl](mailto:s.wahls@tudelft.nl); [m.bruehl@tudelft.nl](mailto:m.bruehl@tudelft.nl)

### 1. Introduction

In the past decade, observations in the German estuaries such as the rivers Elbe and Weser show increasingly serious damage to bank protection structures (groins and revetments). This damage is caused mainly by waves induced by the passing of big container ships in the shallow and narrow maritime waterways. These ship-induced 3D wave fields consist of long-periodic primary and short-periodic secondary wave components. Due to missing design approaches for the load of long-period waves on rubble-mound revetments, the current risk assessment for protective structures in maritime waterways is based on short-period, wind-induced waves. Therefore, the structures do not ensure sufficient stability against the long-period ship-induced wave loads within the estuaries.

Within the research project “Parameterization of nonlinear ship-induced 3D wave fields for the hydraulic design of protective structures in maritime waterways (PaNSiWa)”, we apply nonlinear Fourier transforms (NFTs) on experimentally generated ship waves in maritime waterways. The objective of the project is to provide better understanding of the underlying nonlinear structure of the long-period primary waves and to separate the nonlinear spectral basic components within the ship-wave data from their nonlinear wave-wave interactions. In this paper, we present first analyses of the decomposition of ship-wave measurements from experimental tests and the identification of hidden solitons within the long-period primary ship wave.

### 2. Nonlinear Fourier transform based on the Korteweg-de Vries equation

The KdV equation was proposed by Korteweg and De Vries (1895) to describe the evolution of the free surface  $\eta(x,t)$  of long, progressive, unidirectional surface waves in shallow water (with relation of depth and wave length  $h/L < 0.22$ ) over horizontal bottoms in space and time. For the analysis of periodic time series  $\eta(x_0,t)$  (measured at a fixed position  $x_0$ ) the time-like KdV equation (tKdV) is applied (Karpman 1975; Osborne 1993):

$$\eta_x + c'_0 \eta_t + \alpha' \eta \eta_t + \beta' \eta_{ttt} = 0, \quad \eta(x,t) = \eta(x, t + T_w), \quad (1)$$

where  $\eta(x,t)$  is the free surface elevation as a function of space  $x$  and time  $t$ ,  $\eta_x = \partial \eta / \partial x$  is the vertical velocity of  $\eta(x,t)$ ,  $\eta_t = \partial \eta / \partial t$  is the partial derivative of  $\eta(x,t)$  in time  $t$ ,  $\eta_{ttt}$  is the third-order partial derivative in time  $t$  of  $\eta(x,t)$ ,  $\alpha' \eta \eta_t$  is the nonlinear convective term and  $\beta' \eta_{ttt}$  is the dispersive term. Since periodic travelling-wave conditions are assumed,  $\eta(x,t) = \eta(x, t + T_w)$ , the variable  $t$  is considered within the period interval  $0 \leq t \leq T_w$ . The wave celerity or linear phase speed for the tKdV in shallow-water  $c'_0$ , the coefficients  $\alpha'$  for nonlinearity and  $\beta'$  for dispersion, and the relation  $\lambda'$  between nonlinearity and dispersion are constant parameters that depend on the particular physical application (Osborne 2010, Sect. 10.1, p. 219). For progressive surface waves modelled by the tKdV, these coefficients depend on the water depth  $h_0$  and the acceleration due to gravity  $g$  as follows (Karpman 1973, Osborne 1993):

$$c'_0 = \frac{1}{c_0} = \frac{1}{\sqrt{gh_0}}, \quad \alpha' = -\frac{3}{2c_0 h_0}, \quad \beta' = -\frac{c_0 h_0^2}{6c_0^3}, \quad \lambda' = \frac{\alpha'}{6\beta'} = \frac{3c_0^2}{2h_0^3}. \quad (2)$$

Nonlinear Fourier transform (NFT) is an umbrella term for special signal processing techniques that can analytically solve certain nonlinear evolution equations such as the KdV. In contrast to the conventional linear Fourier transforms (FT), NFTs are able to separate the nonlinear spectral basic components within the free-surface data from their nonlinear interactions. Therefore, NFTs can extract nonlinear features of shallow water waves, such as hidden solitons, which cannot be detected by FT (Brühl 2014; Osborne 2010; Prins and Wahls, 2019). The analysis of shallow-water free-surface wave data by application of the NFT for the solution of the KdV equation is called KdV-NFT.

### 3. Ship-induced long-period primary waves in narrow channels

The BAW (Federal Waterways Engineering and Research Institute, Hamburg, Germany) has conducted extensive hydraulic model tests (scale 1:40) and field measurement to investigate the ship's dynamic performances and ship-induced wave fields. Especially, they conducted experiments to investigate the generation of long-period ship-induced wave fields in very shallow and narrow channel cross-sections (Flügge and Uliczka 2001). The channel cross-section in Fig. 1 shows an experimental set-up with the central ship route in a trapezoidal-shaped channel. For the analysis, we use the measurements of four wave gauges on both sides of the ship as shown in the figure (WGS1-4 and WGB1-4). We filter the measured ship waves by applying a low-pass filter with a cut-off frequency of  $f=0.067$  Hz to separate the short-period secondary wave components from the long-period primary wave.

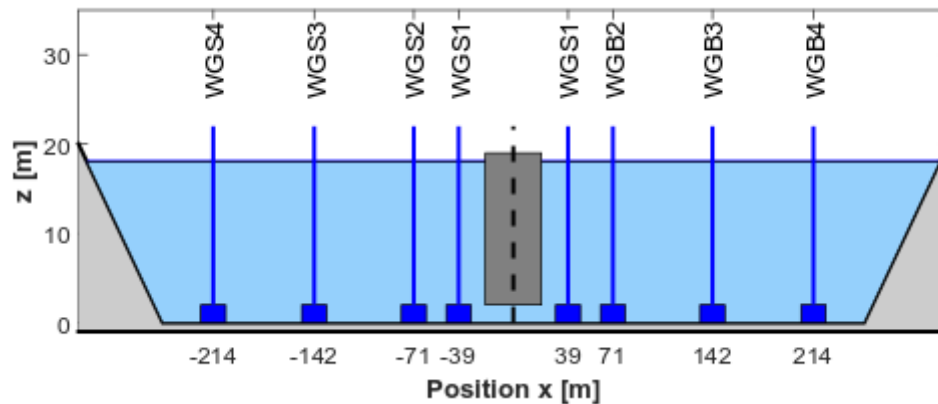


Figure 1. Schematic representation of channel cross-section in the model test with central ship route (in natural scale).

The left column in Fig. 2 exemplarily shows the primary waves at gauges WGS1 to WGS4 (see Fig. 1) after low-pass filtering of the measured free-surface elevation. Observation of the data shows that the primary wave in general can be divided into three different sections: i) A first elevation at the beginning of the signal (red curve in the figure), originating at the bow of the moving ship. ii) A depression along the ship as it passes the wave gauges (green curve). iii) A second elevation after the ship has passed the gauges (blue curve), originating from the stern of the ship.

In this example, the first elevation (red curve in Fig. 2) consists of two peaks. The first peak represents a solitary wave travelling in front of the ship over the whole channel width (Wu 1987). Therefore, this wave shows a nearly constant wave height in all four time series and, thus, is independent of the distance between gauge and ship course. The second peak represents the bow wave generated by the bow of the moving ship. With increasing distance from the ship from WGS1 to WGS4, the amplitude of the second peak is decreasing and the peak is becoming wider. The depth of the depression (green curve) is also decreasing significantly with the distance from the

ship. In this example, the existence of the second elevation (blue curve) depends on the gauge position. Close to the ship, a second elevation is observed (WGS1+2), but not at gauges WGS3+4 further away.

The results in the presented example show that the ship-induced long-period primary waves generated in shallow-water conditions are subject to changes in shape with increasing distance from the ship. Apart from the nearly constant soliton in front of the ship (first peaks in the time series), the height of the peak amplitudes of the first elevation, the number and the elevation of the peaks in the second elevation, and the depth of the depression are decreasing with distance from the moving ship. Nevertheless, as the wave approaches the channel banks the remaining peaks and the depression still can cause significant damage to the bank protection structures.

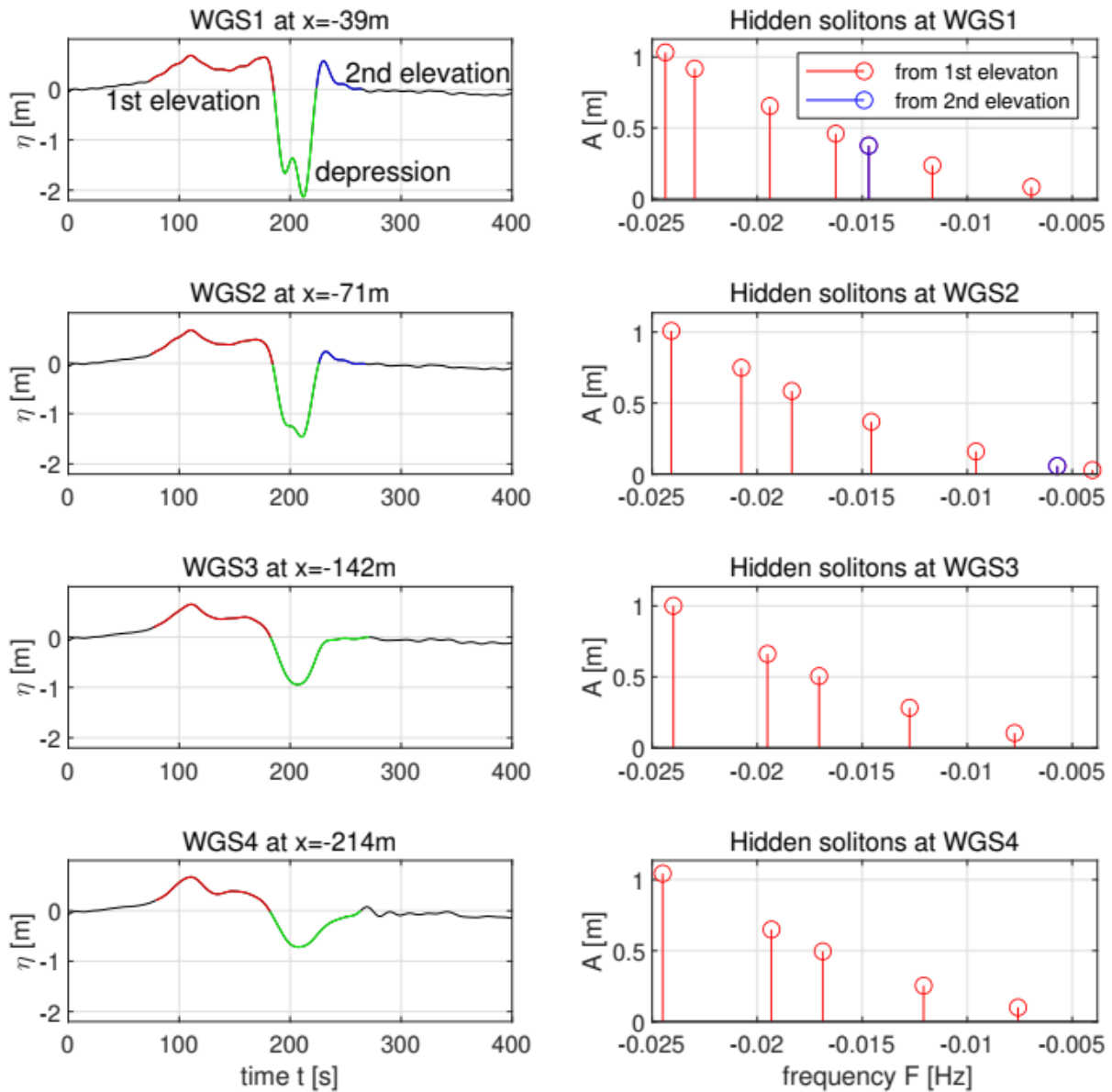


Figure 2. Left columns: long-period ship waves from WGS1-4. Right columns: solitons in KdV-NFT spectra with vanishing boundary conditions (solitons are plotted over negative frequencies)

#### **4. Determination of hidden solitons in the primary ship waves using KdV-NFT**

We know from other experiments and analyses that smooth long-period waves in shallow water such as cosine waves can transform into a train of solitons (Brühl, 2014; Brühl and Oumeraci, Zabusky and Galvin, 1971). Karpman (1975) shows that, based on the initial condition and the relation between nonlinearity and dispersion, an initial perturbation can transform into either only solitons or solitons followed by a tail of rapidly oscillating wave packets. Thus, one of our research objectives is to determine the number and the amplitudes of the solitons that are hidden in the measured primary waves by application of the KdV-NFT. The part of the nonlinear spectrum that contains the oscillatory wave components is not discussed here. At this stage of analysis, we analyse ship-wave data from point measurements so that we can neglect that the ship-wave field is not propagating freely but is bound to the ship and moves with the ship velocity.

Each of the four time series in Fig. 2 are analysed using the KdV-NFT, see for example Osborne (2010) or Prins and Wahls (2019). For each analysis, the right column shows the determined solitons as amplitude-frequency plot. The soliton frequencies given in the plot are not wave frequencies in the classic sense. They refer to the factor in front of the time variable, which is coupled to the amplitude of the solitons (see Brühl et al. (2021) for details). The negative sign is added to separate the solitons from the oscillatory components in the spectrum. For example, the nonlinear analysis of the time series at WGS1 shows that the KdV-NFT spectrum of this primary wave contains seven solitons with amplitudes  $A=1.03, 0.92, 0.65, 0.46, 0.38, 0.24$  and  $0.08$  m. By a short-time analysis (not shown here) where different segments of the time series are analysed individually, the first four and the last two solitons can be attributed to the first elevation (red stems in Fig. 2). The depression part of the primary wave does not provide any solitons in the KdV-NFT. The fourth soliton (blue stem) can be attributed to the second elevation.

A closer look at the solitons from the first elevation (red stems) shows that the amplitude of the largest spectral soliton remains nearly constant in the data from WGS1-4. This is in agreement with the interpretation of the first peak being a solitary wave with constant amplitude over the whole width of the channel. In the time series at WGS1 to WGS4, the first peaks show maximum elevations of about  $0.65$  to  $0.67$  m. The discrepancy to the spectral soliton amplitudes can be attributed to additional nonlinear interactions that lead to a depression of leading solitons. From WGS1 over WGS2 to WGS3, the amplitudes of the next solitons are decreasing and the solitons are shifted to the right in the spectrum. The smallest soliton is only found in WGS1+2, but has disappeared in WGS3+4 as the height of the second peak in the first elevation in the time series has decreased. Since the shape of the first elevation is nearly equal in WGS3+4, also the same number of solitons with nearly the same amplitudes are found in the data. In the second elevation (blue stems), the soliton shows a reduced amplitude in the spectrum and is shifted to the right as the peak elevation decreases from WGS1 to WGS2 until no soliton is found (WGS3+4).

The spectral results show that the KdV-NFT identifies the hidden solitons in the primary wave and determines their numbers and amplitudes. By a nonlinear short-time analysis, the different solitons are attributed to the different elevation parts of the signal. The depression part does not contain any solitons. Furthermore, the numbers and amplitudes change as the shape of the primary waves changes from WGS1 to WGS4. The larger the peak elevations the larger the number of solitons and their amplitudes. This is agreement with the results from previous experiments and literature.

#### **5. Far-field propagation of the primary wave using numerical simulation**

The interpretation of the nonlinear spectra is the following: The analysed data consist of solitons and oscillatory components (not shown here) – and their nonlinear interactions. In the KdV-NFT, the interactions are separated from the spectral wave components and the latter can be identified although they might not be obviously visible in the data. The nonlinear spectra presented here show the solitons that are determined in the data by KdV-NFT. The linear superposition of these solitons and the oscillatory waves (not discussed here) *and* their nonlinear interactions (also not discussed here) returns the analysed free-surface data. Thus, the spectral solitons are not clearly visible in the data, because the observed free surface consists of the superposition of solitons,

oscillatory waves, and their nonlinear wave-wave interactions

We conducted a numerical simulation for the data at WGS1 with sufficient propagation length such that the different celerities of the spectral components (dispersion) lead to a separation of the waves in the far field. The simulation results in Fig. 3 show the numerical gauge data at two different positions. The upper plot present the propagated ship wave at  $x=25$  km in an intermediate state: The leading solitons started to separate from the first elevation, the depression has gone, a clear soliton started to emerge out of the second elevation, and a tail of rapidly oscillating waves has developed. The lower plot shows the far-field situation at  $>x=125$  km. Here, the six solitons that evolved out of the first elevation can be clearly identified as discrete solitons (red curve). The soliton that emerged out of the second elevations (blue curve) is also clearly shown as it starts to overtake the smaller solitons from the first elevation. The oscillatory tail (also denoted as radiation component) originating from the depression is left behind as the solitons propagate faster than the radiation. These results are in agreement with the KdV-NFT analysis at WGS1 presented in Fig. 2.

The numerical far-field results confirm that in fact, a long-period primary ship wave in shallow water contains physically existing solitons. Furthermore, the KdV-NFT is able to reliably identify these solitons from the measured data. These results are in accordance with the findings in Karpman (1975). In this example, the initial smooth long-period shallow-water wave transforms into solitons and an oscillatory tail (see Fig. 3).

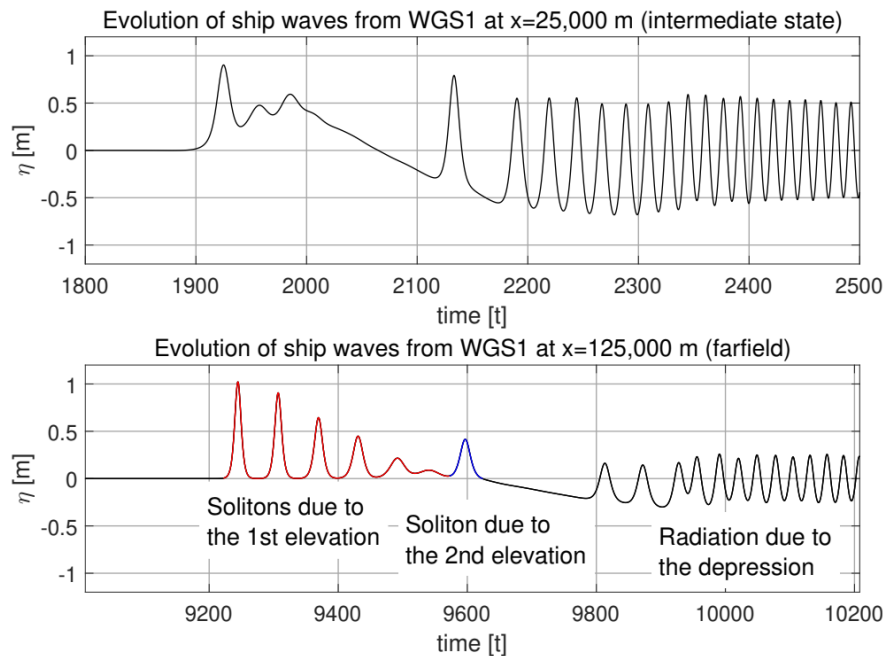


Figure 3. COULWAVE simulation. The solitons detected by KdV-NFT emerge after long propagation.

## 6. Summary

Long-period ship-induced primary waves in narrow channels are generated in relatively shallow water depth. Therefore, we can assume the KdV equation to be applicable for the analysis of these waves, at least if we ignore the external forcing by the moving ship. The nonlinear analysis of primary waves from experimental tests using KdV-NFT as presented here shows that the different elevation parts of the primary wave contains solitons. In contrast, the depression does not show any solitons. These results confirm the findings in Hammack and Segur (1974) and Karpman (1975) whereupon a wave packet consisting of a bump followed by a depression (similar to the long-period ship wave) can transform into solitons (and an oscillatory tail). A numerical simulation has confirmed that in the far field the solitons determined by KdV-NFT will emerge out of the

elevation parts of the primary wave (followed by an oscillating tail).

With increasing distance from the ship, the shape of the primary wave becomes smoother and the peak elevations of bow and stern waves and the depth of the depression decrease. In analogy to the transformation of the primary wave, the number of spectral solitons and their amplitudes decrease with increasing distance to the ship.

Based on these results, we can consider the KdV-NFT to be a helpful tool for the nonlinear analysis of long-period primary ship waves. The analysis of further experimental data will help to characterize different wave patterns based on nonlinear spectral parameters. Furthermore, we will analyse the transformation of the primary wave from the ship to the shore based on KdV-NFT results.

### Acknowledgements

The project PaNSiWa is funded by Deutsche Forschungsgemeinschaft (German Research Foundation, DFG BR 5289/2-1). This project has received funding from the European Research Council (ERC) under the European Union's Horizon 2020 research and innovation programme (grant agreement No 716669).

### References

- Brühl, M. 2014. Direct and inverse nonlinear Fourier transform based on the Korteweg–de Vries equation (KdV-NLFT) – A spectral analysis of nonlinear surface waves in shallow water. Dissertation. Technische Universität Braunschweig. Braunschweig, Germany
- Brühl, M. and H. Oumeraci (2016). Analysis of long-period cosine-wave dispersion in very shallow water using nonlinear Fourier transform based on KdV equation. *Applied Ocean Research* Vol. 61: 81-91.
- Brühl, M., P. J. Prins, S. Ujvary, I. Barranco, S. Wahls and P. L.-F. Liu (2021). Comparative analysis of bore propagation over long distances using conventional linear and KdV-based nonlinear Fourier transform. (submitted).
- Flügge, G. and Ulizka, K. 2001. Fahrverhalten großer Containerschiffe in extrem flachem Wasser. *HANSA*, 138. Jahrg. Nr. 12.
- Hammack, J. L. and H. Segur (1974). The Korteweg-de Vries equation and water waves. Part 2. Comparison with experiments. *J. Fluid Mech.* Vol. 65: pp. 289-314.
- Karpman, V. I. (1975). *Non-linear Waves in Dispersive Media*. Oxford, Pergamon.
- Korteweg, D. J. and G. deVries (1895). On the change of form of long waves advancing in a rectangular canal, and on a new type of long stationary waves. *Philos. Mag. Ser. 5(39)*: pp. 422-443.
- Osborne, A. R. (1993). The behaviour of Solitons in Random-Function Solutions of the Periodic Korteweg-deVries Equation. *Physical Review Letters* vol. 71(no. 19): pp. 3115-3118.
- Osborne, A. 2010. *Nonlinear Ocean Waves and the Inverse Scattering Transform*, Vol. 97. Academic Pr.
- Prins, P. and Wahls, S. 2019. Soliton phase shift calculation for the Korteweg–de Vries equation. *IEEE Access*, 7, 122914-122930.
- Wu, Y.-T. (1987). Generation of upstream advancing solitons by moving disturbances. *J. Fluid Mech.* 184: 75-99.
- Zabusky, N. J. and C. J. Galvin (1971). Shallow-water waves, the Korteweg-deVries equation and solitons. *J. Fluid Mech.* 47(4): pp. 811-824.